Anisotropic optical emission of single CdSe/CdS tetrapod heterostructures: Evidence for a wavefunction symmetry breaking

C. Mauser, T. Limmer, E. Da Como,* K. Becker, A. L. Rogach, and J. Feldmann
Photonics and Optoelectronics Group, Physics Department and CeNS, Ludwig-Maximilians-Universität, Amalienstrasse 54, 80799 Munich, Germany

D. V. Talapin
Department of Chemistry, The University of Chicago, Chicago, Illinois 60637, USA
(Received 6 March 2008; published 15 April 2008)

Semiconductor tetrapods are expected to exhibit isotropic optical properties due to their tetrahedral symmetry. We have investigated the optical polarization properties of individual CdSe/CdS tetrapods of high structural quality. In contrast to the light absorption behavior, a pronounced anisotropy is observed in the optical emission. This unexpected result can only be explained by assuming a symmetry breaking in the electronic wavefunction. Calculations reveal that slight differences between the arm diameters induce the polarized emission and a decrease in the photoluminescence intensity.

DOI: 10.1103/PhysRevB.77.153303 PACS number(s): 78.67.Bf, 61.46.Hk, 73.22.Dj

Tetrapods are a class of colloidal nanocrystals exploiting the polytipism of the group II-VI semiconductors to generate branched nanostructures with a tetrahedral symmetry.[1,2] The three dimensional (3D) morphologies formed by such materials have a huge potential to couple and implement quantum confined semiconductors in electronic and optoelectronic devices such as single quantum dot transistors[3] and photovoltaic cells.[4] While the combination of different types of material is feasible,[2,5] opening the way to heterostructures with a spatially controlled energy landscape,[2] the role of shape and size in tuning the electronic structure remains largely unexplored. The main reason resides in the intrinsic challenges of accessing the wavefunction distribution in such 3D nano-objects avoiding perturbing probes. A detailed mapping of the electronic properties and wavefunction symmetry will allow the design and control of quantum confinement by tuning the shape along the preferential directions.

Here, we report a single-particle spectroscopy study on semiconductor tetrapods. Considering CdSe/CdS heterostructures, we probed the electron wavefunction spatial distribution across the branching point of these nanostructures. Polarization sensitive detection reveals that over 80% of the tetrapods are emitting light with a preferable polarization. This unexpected result, for a supposedly symmetric structure, is interpreted considering a symmetry breaking in the electron wavefunction. Model calculations show the major role played by the lateral dimension of the arms in tuning the quantum confinement and demonstrate how an asymmetry in the diameter of one arm causes the electron wavefunction localization in this direction. The asymmetry is not only responsible for the polarized emission but it also tunes the photoluminescence (PL) intensity, as the electron wavefunction localization decreases the overlap with the core centered hole.

The recently introduced seeded growth allows for the preparation of luminescent tetrapod heterostructures containing a CdSe core and CdS arms.[5] On the four characteristic (111) facets of the zinc-blende CdSe core, CdS arms are grown with a wurtzite structure. A representative transmission electron microscopy (TEM) image of such a tetrapod-shaped nanocrystal is shown in Fig. 1(a). The inset shows a lower magnification TEM image for a differently oriented tetrapod. In Fig. 1(b), the absorption (solid line) and PL (dashed line) spectra of the tetrapods dispersed in a toluene solution illustrate the ensemble optical properties. The absorption spectrum is dominated by the extinction band starting at 500 nm due to the four CdS arms.[5] The absorption features assigned to the CdSe core can be identified at 630 nm (inset). The emission spectrum suggests charge recombination in the CdSe core, in a similar way to the previously investigated CdSe/CdS core/elongated shell nanorods.[6] In contrast to conventional CdSe or CdTe-only tetrapods, the peculiar band-edge energy level alignment of our heterostructure maintains the hole confined in the spherical CdSe core allowing for the delocalization of the electron in the almost degenerate CdSe/CdS conduction bands.[5,7] This energy band engineering assures a high PL efficiency[5] (50% at room temperature) and elects these nanocrystals as an ideal model system for the study of electron wavefunction distribution and symmetry by single-particle PL spectroscopy.

Single-particle measurements were performed by imaging isolated tetrapods dispersed in a 50 nm thick polymer matrix (Zeonex) with a home built wide-field fluorescence microscope equipped with a liquid helium cryostat.[6] The PL was excited with a cw argon ion laser (458 nm, 2 W/cm^2) and detected with a charge-coupled device camera coupled to a spectrograph. The histogram (orange columns), superimposed on the ensemble PL spectrum of Fig. 1(b), illustrates the distribution of the PL emission energy peaks of 170 single tetrapods at room temperature. The well matched profile of the ensemble spectrum reveals the potential of single-particle measurements in extracting the spectroscopical properties of the tetrapods avoiding inhomogeneous broadening.

In the last years, single-particle spectroscopy by using polarized light gave remarkable insights into the comprehension of the electronic structure in spherical and elongated semiconductor nanocrystals.[8,9] For our study, we first consid-

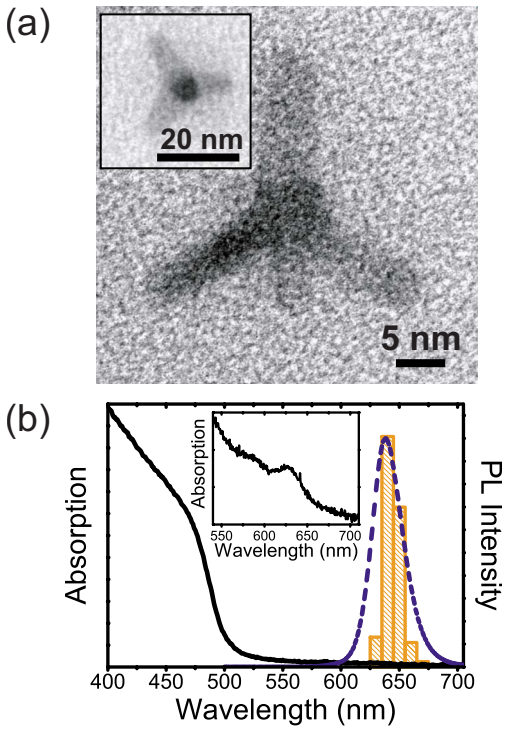

FIG. 1. (Color online) (a) TEM image of a single CdSe/CdS tetrapod. The average value for the diameter of the core is estimated to be in the range of 4–6 nm. The arm length can vary from 14 to 20 nm. The inset shows a lower magnification image of a tetrapod oriented with one arm perpendicular to the surface. (b) Room temperature absorption (solid black line) and PL (dashed blue line) spectra of a dilute solution of tetrapods in toluene. The inset shows the absorption band (630 nm) ascribed to the CdSe core. Orange (light gray) columns represent a histogram of the emission energy peaks obtained from the room temperature PL spectra of 170 single tetrapods.

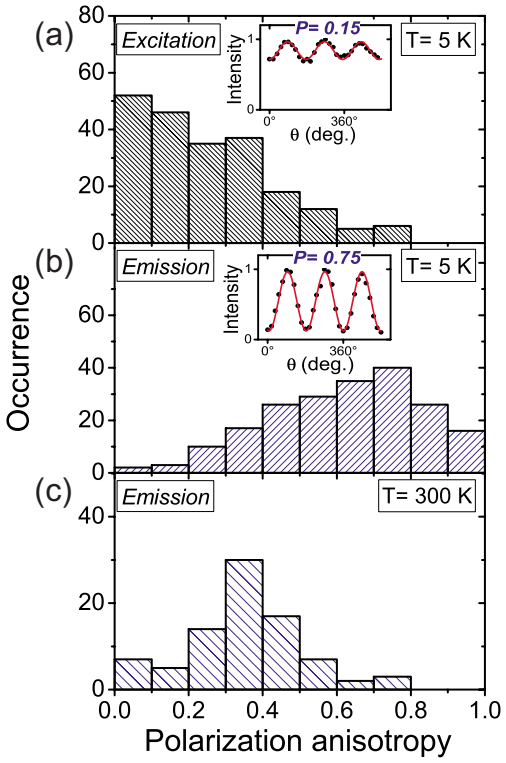

FIG. 2. (Color online) Polarization anisotropy histograms in (a) excitation, (b) emission at low temperature ($T=5$ K), and (c) emission at room temperature ($T=300$ K). The insets in (a) and (b) show the examples of polarization anisotropy traces for two different tetrapods in excitation and emission, respectively. The red (dark gray) lines represent fitting of the experimental data (black dots) with a $\cos^2\theta$ function. The extracted anisotropy values are 0.15 and 0.75 for excitation and emission, respectively.

ered the polarization anisotropy in excitation, which is measured by rotating a $\lambda/2$ plate placed in the exciting laser beam path and recording the PL intensity (I) of single tetrapods as a function of the light polarization angle θ. An anisotropy parameter, defined as $P=(I_{max}-I_{min})/(I_{max}+I_{min})$, was extracted from the intensity traces $I(\theta)$ [an example is reported in the inset of Fig. 2(a) resulting in $P=0.15$]. Figure 2(a) reports a histogram of P for a total of 200 single tetrapods at low temperature (5 K), which peaks at $P=0$ and shows a continuously decreasing probability for higher values. This result is consistent with a large amount of particles characterized by an unpolarized absorption and can be described considering that optical excitation, involving the CdS arms, gives slightly different anisotropies (from 0 to 0.14) according to the tetrapod orientation with respect to the laser propagation. Considering the laser impinging perpendicular to the substrate, $P=0$ is expected for the orientation in the *inset* of Fig. 1(a), whereas an increased absorption probability ($P=0.14$) characterizes the orientation with the two vertical collinearly projected arms [see Fig. 1(a)]. The decreasing amount of tetrapods displaying values beyond 0.2 indicates the presence of potentially distorted tetrahedral geometries. Of these, only a small subset of particles (5%) with a lost tetrapod shape, such as nanorods, was revealed by a detailed statistical TEM analysis.

In a second experiment, we studied the anisotropy in the emitted PL [Fig. 2(b)] obtained by rotating a polarizer in the light emission path after circularly polarized excitation. Remarkably, we observe an almost mirrored histogram with respect to excitation, showing the most probable values peaking at 0.7. This result suggests that the process of electron-hole recombination takes place for a well-defined polarization, without changes in phase during the course of the measurement [see an emission anisotropy trace in the Fig. 2(b), inset]. More than 50% of the tetrapods show $P>0.5$, demonstrating an unexpected behavior for a large number of such highly symmetric nanostructures. The same type of measurement performed at room temperature [Fig. 2(c)] shows the emission anisotropy shifting to lower values (peak at 0.3). While this observation can be explained by the thermal population of higher energy states with different symmetries with respect to the band edge, it also excludes that the emission anisotropy is due to an underestimated amount of rods, the latter being characterized by an almost temperature-independent anisotropy.[10]

In order to shed light on the physical phenomenon responsible for the experimentally observed anisotropies, we modeled the emitting electronic states by using a semiempirical

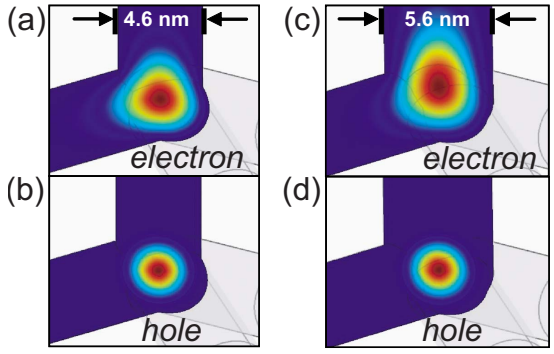

FIG. 3. (Color online) Color contour plots for the normalized electron and hole wavefunction distribution probability for [(a) and (b)] symmetric and (c) and (d) asymmetric tetrapods, respectively. The asymmetry is induced by increasing the diameter of one arm by 1 nm. The wavefunction distribution is plotted on a plane parallel to two arms and containing the center of the CdSe core.

approach based on an effective mass approximation.[7,11] Although, such a theoretical description is not appropriate for a quantitative estimation of the energy level ordering, particularly for higher lying states,[12,13] it can offer an accurate prediction of the wavefunction delocalization in heterostructures, as was previously demonstrated for CdSe/CdS nanorods.[7] We started considering the band-edge states in the case of a perfectly symmetric tetrapod [Figs. 3(a) and 3(b)]. The color contour plots show the normalized electron and hole wavefunction densities in a plane parallel to two arms and intersecting the CdSe core. Because of the valence band offset of our heterostructure, during charge carrier relaxation to the band edge, the hole confines in the CdSe core, whereas the electron wavefunction shows a certain probability of symmetrically penetrating in the four CdS arms [Fig. 3(a)]. The equal probability of electron-hole recombination in all the four directions for such perfectly symmetric tetrapods leads to unpolarized emission, which is almost not observed in the statistics of Fig. 2(b). We deliberately induced asymmetric variations in the shape, such as a longer or a wider arm, which are both consistent with growth-related phenomena.[1,5] While a mere increase in the length of one arm provokes a negligible asymmetry in the electron and hole wavefunctions, an increase in diameter width by 1 nm induces a symmetry breaking in the electron wavefunction with a consequent localization along this direction [Fig. 3(c)]. Our model, identifying the predominant role played by the arm diameter in controlling the quantum confinement, not only agrees with the previous studies on tetrapods,[1,13] but it also provides a straightforward explanation to the experimental findings. Here, we restrict our discussion to the simplest case where only one arm over the entire tetrapod structure was modified, although we do not exclude that more complex structures involving diameter variations in more than one arm are possible, making up the large distribution of P observed in Fig. 2(b). Previous studies on the anisotropy of nanorods considered the role of dielectric confinement for describing the observed anisotropies.[14,15] This effect would eventually enhance the intrinsic anisotropy and was taken into account for fitting the anisotropy traces of nanorods.[15] In our experiments, all tetrapods are homogeneously dispersed

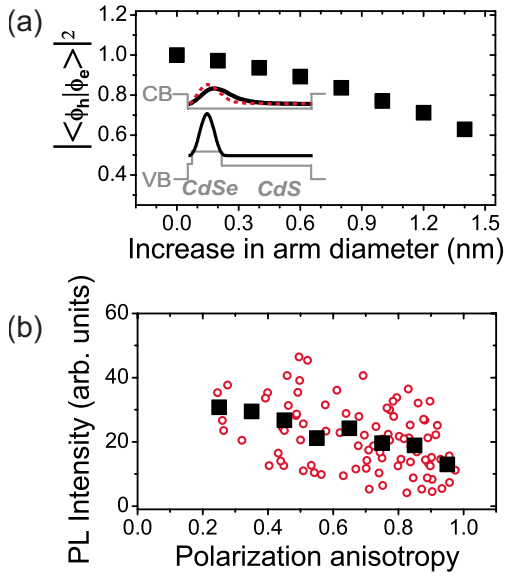

FIG. 4. (Color online) (a) Plot of the calculated squared wavefunction overlap integral $|\langle\phi_e|\phi_h\rangle|^2$ against the increase in the diameter of one arm. The inset shows a cross section of the electron and hole wavefunctions in the conduction and valence bands along the modified arm for increases of 0 (red dashed curve) and 1 nm (black curve) in the diameter. (b) Measured scatter plot of PL intensity as a function of polarization anisotropy for 90 single tetrapods (circles); the squares are obtained after averaging single tetrapods with a binning of 0.1 in polarization anisotropy.

in a common polymer matrix, virtually sampling the same dielectric medium. Since the histograms of Fig. 2 show the presence of tetrapods within the full range of possible P, the anisotropy must be mainly controlled by wavefunction confinement effects, as further confirmed by the temperature behavior observed in Figs. 2(b) and 2(c).

We exclude that the observed linearly polarized emission is influenced by the presence of surface charges created upon high power optical excitation.[6,16] As observed in nanorods and in nanowires,[6,17] surface charges, ascribed to electrons, should diffuse upon the surface of the four arms. Considering a role of the electrons in generating a polarizing electric field, the diffusion must cause a switching in the phase of the anisotropy trace. We did not observe any evidence of switching of the phase for all the studied tetrapods (more than 500). Moreover, all the experiments were performed at low excitation power (2 W/cm^2) resulting in undetectable surface-charge induced phenomena, such as PL blinking.[16,18]

In quantum confined nanostructures, the PL radiative rate is proportional to the electron-hole wavefunction overlap.[7,19] In the case of tetrapods displaying polarized emission, the electron localization along one arm should decrease the wavefunction overlap with the hole which remains confined in the core [Figs. 3(c) and 3(d)]. Figure 4(a) shows how an increase in the arm diameter influences the normalized overlap integral $|\langle\phi_e|\phi_h\rangle|^2$. The inset of Fig. 4(a) illustrates the change in electron wavefunction distribution along the *asymmetric arm* for increases in diameter of 0 (red dashed curve) and 1 nm (black curve). According to these theoretical predictions, we expect that tetrapods with a pronounced aniso-

tropy *will less efficiently emit* with respect to the ones emitting unpolarized light. Figure 4(b) shows the experimental results summarizing a correlation between the integrated PL intensity and the polarization anisotropy for a total of 90 single tetrapods (circles). Although the data widely scatter, a clear correlation exists between PL intensity and the degree of asymmetry. Binning of data points over anisotropy intervals of 0.1 (squares) results in a clear trend of how the electron wavefunction localization controls the PL intensity. Assuming that the PL intensity is mainly controlled by the radiative rate allows us to estimate the modulation in the arm diameter to induce certain anisotropy. Restricting to the case of only one arm contributing to the electron localization, we can extract the relative change in the arm diameter in order to obtain the observed decrease of about 30% in the emission intensity. The values span a range which is in remarkable agreement with the diameter variance obtained from the seeded growth process[5] and observed in the TEM images [Fig. 1(a)].

In conclusion, we probed the electron and hole wavefunction spatial distribution in luminescent CdSe/CdS tetrapod heterostructures by single-particle light-polarized spectroscopy. A statistical analysis of the emission anisotropy reveals a large amount of single tetrapods emitting linearly polarized light. This result is described by an effective mass model which visualizes the *symmetry breaking and localization* of the electron wavefunction along the tetrapod arm with the larger diameter. These properties, combined with the giant absorption cross sections,[5] suggest a possible application in photonic devices where diffuse light has to be harvested and concentrated toward a specific direction. Additionally, this work shows how the unexpected anisotropic properties of tetrapods can be enhanced by a fine tuning of the lateral quantum confinement along one of the four directions across the branching point. Moreover, the statistical presence of tetrapods with asymmetric properties is expected to have important implications for the implementation of such nanostructures in optoelectronic and electronic nanoscale devices. For example, single-tetrapod devices are expected to transfer electrons or excitons across the branching point; wavefunction localization could be critical for their operation.

J.F., A.L.R., and D.V.T. are grateful to the German Excellence Initiative for funding via the "Nanosystems Initiative Munich (NIM)" and the "LMUexcellent" program.

*enrico.dacomo@physik.uni-muenchen.de

[1] L. Manna, D. J. Milliron, A. Meisel, E. C. Scher, and A. P. Alivisatos, Nat. Mater. **2**, 382 (2003).
[2] D. J. Milliron, S. M. Hughes, Y. Cui, L. Manna, J. B. Li, L. W. Wang, and A. P. Alivisatos, Nature (London) **430**, 190 (2004).
[3] Y. Cui, U. Banin, M. T. Björk, and A. P. Alivisatos, Nano Lett. **5**, 1519 (2005).
[4] B. Q. Sun, E. Marx, and N. C. Greenham, Nano Lett. **3**, 961 (2003).
[5] D. V. Talapin, J. H. Nelson, E. V. Shevchenko, S. Aloni, B. Sadtler, and A. P. Alivisatos, Nano Lett. **7**, 2951 (2007).
[6] J. Müller, J. M. Lupton, A. L. Rogach, J. Feldmann, D. V. Talapin, and H. Weller, Phys. Rev. Lett. **93**, 167402 (2004).
[7] J. Müller, J. M. Lupton, P. G. Lagoudakis, F. Schindler, R. Koeppe, A. L. Rogach, J. Feldmann, D. V. Talapin, and H. Weller, Nano Lett. **5**, 2044 (2005).
[8] N. Le Thomas, E. Herz, O. Schops, and U. Woggon, Phys. Rev. Lett. **94**, 016803 (2005).
[9] J. T. Hu, L. S. Li, W. D. Yang, L. Manna, L. W. Wang, and A. P. Alivisatos, Science **292**, 2060 (2001).
[10] X. Z. Li and J. B. Xia, Phys. Rev. B **66**, 115316 (2002).
[11] A semiempirical model was iterated for the electron and hole wavefunctions following a Hartree approach and considering a single particle picture with an effective potential counting for the Coulomb interaction. The effective masses for the materials were $mh^*(\mathrm{CdSe})=0.45$, $me^*(\mathrm{CdSe})=0.13$, $mh^*(\mathrm{CdS})=0.7$, and $me^*(\mathrm{CdS})=0.18$.
[12] L. W. Wang and A. Zunger, J. Phys. Chem. B **102**, 6449 (1998).
[13] J. B. Li and L. W. Wang, Nano Lett. **3**, 1357 (2003).
[14] J. F. Wang, M. S. Gudiksen, X. F. Duan, Y. Cui, and C. M. Lieber, Science **293**, 1455 (2001).
[15] A. Shabaev and A. L. Efros, Nano Lett. **4**, 1821 (2004).
[16] S. A. Empedocles, D. J. Norris, and M. G. Bawendi, Phys. Rev. Lett. **77**, 3873 (1996).
[17] V. Protasenko, S. Gordeyev, and M. Kuno, J. Am. Chem. Soc. **129**, 13160 (2007).
[18] M. Nirmal, B. O. Dabbousi, M. G. Bawendi, J. J. Macklin, J. K. Trautman, T. D. Harris, and L. E. Brus, Nature (London) **383**, 802 (1996).
[19] H. J. Polland, L. Schultheis, J. Kuhl, E. O. Gobel, and C. W. Tu, Phys. Rev. Lett. **55**, 2610 (1985).